DOI:
10.1093/eurheartj/ehz100

Document Version
Publisher's PDF, also known as Version of record

ESC European Society of Cardiology

European Heart Journal (2019) **40**, 2290–2299
doi:10.1093/eurheartj/ehz100

FASTTRACK CLINICAL RESEARCH
Imaging

Associations between vascular risk factors and brain MRI indices in UK Biobank

Simon R. Cox[1,2,3]*, Donald M. Lyall[3,4], Stuart J. Ritchie[1,2,5], Mark E. Bastin[1,3,6], Mathew A. Harris[7], Colin R. Buchanan[1,2,3], Chloe Fawns-Ritchie[1,2], Miruna C. Barbu[7], Laura de Nooij[7], Lianne M. Reus[8], Clara Alloza[7], Xueyi Shen[7], Emma Neilson[7], Helen L. Alderson[9], Stuart Hunter[9], David C. Liewald[1,2], Heather C. Whalley[7], Andrew M. McIntosh[1,7], Stephen M. Lawrie[7], Jill P. Pell[4], Elliot M. Tucker-Drob[10], Joanna M. Wardlaw[1,3,6,11], Catharine R. Gale[1,2,12], and Ian J. Deary[1,2]

[1]Centre for Cognitive Ageing and Cognitive Epidemiology, The University of Edinburgh, 7 George Square, Edinburgh, EH8 9JZ, UK; [2]Department of Psychology, The University of Edinburgh, 7 George Square, Edinburgh, EH8 9JZ, UK; [3]Scottish Imaging Network, A Platform for Scientific Excellence (SINAPSE) Collaboration, 300 Bath St, Glasgow, G2 4LH, UK; [4]Institute of Health and Wellbeing, University of Glasgow, 1 Lilybank Gardens, Glasgow, G12 8RZ, UK; [5]Social, Genetic and Developmental Psychiatry Centre, Institute of Psychiatry, Psychology and Neuroscience, King's College London, De Crespigny Park, Denmark Hill, London, SE5 8AF, UK; [6]Brain Research Imaging Centre, Neuroimaging Sciences, The University of Edinburgh, Chancellor's Building, 49 Little France Crescent, Edinburgh, EH16 4SB, UK; [7]Division of Psychiatry, The University of Edinburgh, Kennedy Tower, Royal Edinburgh Hospital, Morningside Park, Edinburgh, EH10 5HF, UK; [8]Alzheimer Centre Amsterdam, Department of Neurology, Amsterdam Neuroscience, VU University Amsterdam, Amsterdam UMC, De Boelelaan 1117, 1081 HV Amsterdam, The Netherlands; [9]NHS Lothian, Waverley Gate, 2-4 Waterloo Place, Edinburgh, EH1 3EG, UK; [10]Department of Psychology, University of Texas, 108 E Dean Keeton St, Austin, Texas 78712, USA; [11]UK Dementia Research Institute at the University of Edinburgh, Edinburgh BioQuarter, Edinburgh, EH16 4UX, UK; and [12]MRC Lifecourse Epidemiology Unit, University of Southampton, Southampton General Hospital, Tremona Road, Southampton, SO16 6YD, UK

Received 8 January 2019; revised 23 January 2019; editorial decision 13 February 2019; accepted 19 February 2019; online publish-ahead-of-print 11 March 2019

Aims Several factors are known to increase risk for cerebrovascular disease and dementia, but there is limited evidence on associations between multiple vascular risk factors (VRFs) and detailed aspects of brain macrostructure and microstructure in large community-dwelling populations across middle and older age.

Methods and results Associations between VRFs (smoking, hypertension, pulse pressure, diabetes, hypercholesterolaemia, body mass index, and waist–hip ratio) and brain structural and diffusion MRI markers were examined in UK Biobank ($N = 9722$, age range 44–79 years). A larger number of VRFs was associated with greater brain atrophy, lower grey matter volume, and poorer white matter health. Effect sizes were small (brain structural R^2 ≤1.8%). Higher aggregate vascular risk was related to multiple regional MRI hallmarks associated with dementia risk: lower frontal and temporal cortical volumes, lower subcortical volumes, higher white matter hyperintensity volumes, and poorer white matter microstructure in association and thalamic pathways. Smoking pack years, hypertension and diabetes showed the most consistent associations across all brain measures. Hypercholesterolaemia was not uniquely associated with any MRI marker.

Conclusion Higher levels of VRFs were associated with poorer brain health across grey and white matter macrostructure and microstructure. Effects are mainly additive, converging upon frontal and temporal cortex, subcortical structures, and specific classes of white matter fibres. Though effect sizes were small, these results emphasize the vulnerability of brain health to vascular factors even in relatively healthy middle and older age, and the potential to partly ameliorate cognitive decline by addressing these malleable risk factors.

Keywords Vascular risk • Brain • MRI • Diffusion • White matter • Cortex

* Corresponding author. Tel: 44 (0)131 650 8493, Email: simon.cox@ed.ac.uk

Introduction

With an increasingly ageing population, it is important to understand the neurobiological underpinnings of age-related cognitive impairment.[1–3] The functional sequelae of age-related cerebral decline carry a high financial, personal, and societal burden, including impaired daily activities,[4,5] predict poorer health, and herald dementia, illness, and death.[6] Dementia costs the UK more than £18 billion per year,[7] and around 1% of global gross domestic product in 2010.[8] The functional consequences of non-pathological brain ageing (which are much more prevalent than dementia) impose serious limitations on independence and quality of life in older age.[9,10] Efforts to understand the determinants of cerebral decline and quantify specific brain effects are urgently needed, especially with respect to modifiable factors which offer relatively direct pathways to intervention.[1,8,10]

Neurovascular health is an important correlate of preserved cognition in adult ageing,[11,12] yet significant gaps remain in our understanding of the links between vascular and cerebral ageing. Cerebral small vessel disease (CSVD; a constellation of clinical and imaging findings of presumed vascular aetiology[13]) causes ~45% of dementia and 20% of stroke worldwide,[14] though its pathophysiology and the interplay among its many possible determinants are not well understood.[13] Though the specific mechanisms by which these determinants, often known as vascular risk factors (VRFs), remain to be fully elucidated, anthropometric indices (waist–hip ratio and body mass index; WHR and BMI), blood glucose, elevated pulse pressure, chronic hypertension, diabetes, and hypercholesterolaemia are all putative VRFs that have been associated with cerebrovascular complications.[15–18] The resultant damage to cerebral vasculature and increased vascular resistance are thought to deregulate cerebral blood flow, alongside blood brain barrier dysfunction, and could further lead to abnormal protein synthesis and formation of Alzheimer's disease-typical plaques and tangles.[15,18,19]

In community-dwelling samples, the comparative importance of separate VRFs for the brain in relatively healthy ageing is unclear. Recent studies have reported brain–heart associations using modern MRI techniques, identifying areas which modulate sympathetic and parasympathetic systems.[20,21] Large-scale comprehensive research designs are required to identify specifically which brain biomarkers are most sensitive to potential VRF effects, yet such data is scarce. Inconsistencies in the extant literature (e.g. discussed in Ref.[22]) may be partly down to low statistical power due to small sample sizes, and consideration of only one or few measures of risk and/or single brain MRI outcomes at any one time.[22] In non-pathological samples, effects are likely to be relatively subtle; well-powered, detailed MRI with multi-tissue analyses which can also account for multiple risk factors (and their tendency to co-occur) have been called for.[23]

UK Biobank represents one of the largest general population cohorts to have collected large-scale brain imaging data alongside information on VRFs among adults in middle and older age. This study examines total burden of vascular risk on global and regional measures of brain grey and white brain matter, derived from structural and diffusion MRI (dMRI) data in UK Biobank participants. We quantify the unique contributions to global and regional brain structure made by each simultaneously modelled VRF. The wide age range further allows us to test the hypothesis that different VRFs may be more important for brain structure in midlife than in later life.[24–26]

Methods

Materials and procedure

When attending the assessment centre for an MRI scan, participants also provided demographic, health, and socioeconomic information in response to a series of touchscreen questions. To improve accuracy, they also took part in a nurse-led interview about their medical history, which included any self-reported diagnoses (http://biobank.ctsu.ox.ac.uk/crystal/field.cgi?id=200). Participants were excluded from the present analysis if they reported having received a diagnosis of dementia, Parkinson's disease or any other chronic degenerative neurological problem (including demyelinating diseases), brain cancer, brain haemorrhage, brain abscess, aneurysm, cerebral palsy, encephalitis, head injury, nervous system infection, head or neurological injury, or trauma, stroke ($N = 210$). A total of 9722 participants provided brain MRI scan data following exclusions, and automated and visual quality control (QC) by UK Biobank Imaging group.

Vascular risk factors

During medical history interview at the brain imaging appointment, participants also reported whether they had received a diagnosis of diabetes, hypertension, or hypercholesterolaemia. Data on cigarette smoking were also available from the touchscreen questionnaire. Blood pressure was collected twice, moments apart, using an Omron 705IT monitor. Pulse pressure was calculated as the log-transformed difference between mean systolic and mean diastolic pressure (or a single measure of each, where two were unavailable). Anthropometric measures were taken after participants had removed bulky clothing and shoes. Waist and hip measurements were conducted to provide WHR, and BMI was calculated as weight (kg)/height^2 (m). For self-reported data, those who preferred not to answer or did not know were excluded from the analysis in all cases (<5%).

MRI acquisition and processing

All brain MRI data were acquired on the same 3T Siemens Skyra scanner, according to a freely available protocol (http://www.fmrib.ox.ac.uk/ukbiobank/protocol/V4_23092014.pdf), documentation (http://biobank.ctsu.ox.ac.uk/crystal/docs/brain_mri.pdf), and publication.[27] In brief, the data were acquired with a standard Siemens 32-channel head coil. T_1-weighted MPRAGE and T_2-weighted FLAIR volumes were acquired in sagittal orientation at $1 \times 1 \times 1$ mm and $1.05 \times 1 \times 1$ mm resolution, respectively. The dMRI acquisition comprised a spin-echo echo-planar sequence with 10 T_2-weighted ($b \approx 0$ s mm^{-2}) baseline volumes, 50 $b = 1000$ s mm^{-2} and 50 $b = 2000$ s mm^{-2} diffusion weighted volumes, with 100 distinct diffusion-encoding directions and 2 mm isotropic voxels. The global tissue volumes, and white matter tract-averaged water molecular diffusion indices were processed by the UK Biobank team and made available to approved researchers as imaging-derived phenotypes (IDPs); the full details of the image processing and QC pipeline are available in an open access article.[27] These included total brain volume, grey matter volume, white matter hyperintensity (WMH) volume, subcortical volumes (accumbens, amygdala, caudate, hippocampus, pallidum, putamen, thalamus), and tract-averaged fractional anisotropy (FA) and mean diffusivity (MD) of the following white matter tracts: acoustic radiation, anterior thalamic, cingulum gyrus, and parahippocampal, corticospinal, forceps major and minor, inferior fronto-occipital, inferior longitudinal, middle cerebellar peduncle, medial lemniscus, posterior thalamic, superior longitudinal, superior thalamic, uncinate. Extreme outlying data points [further than ±4 SD from the mean were excluded case-wise (representing 0.001% of the total IDP data points analysed]. *Figure 1* shows the white matter tracts and subcortical structures.

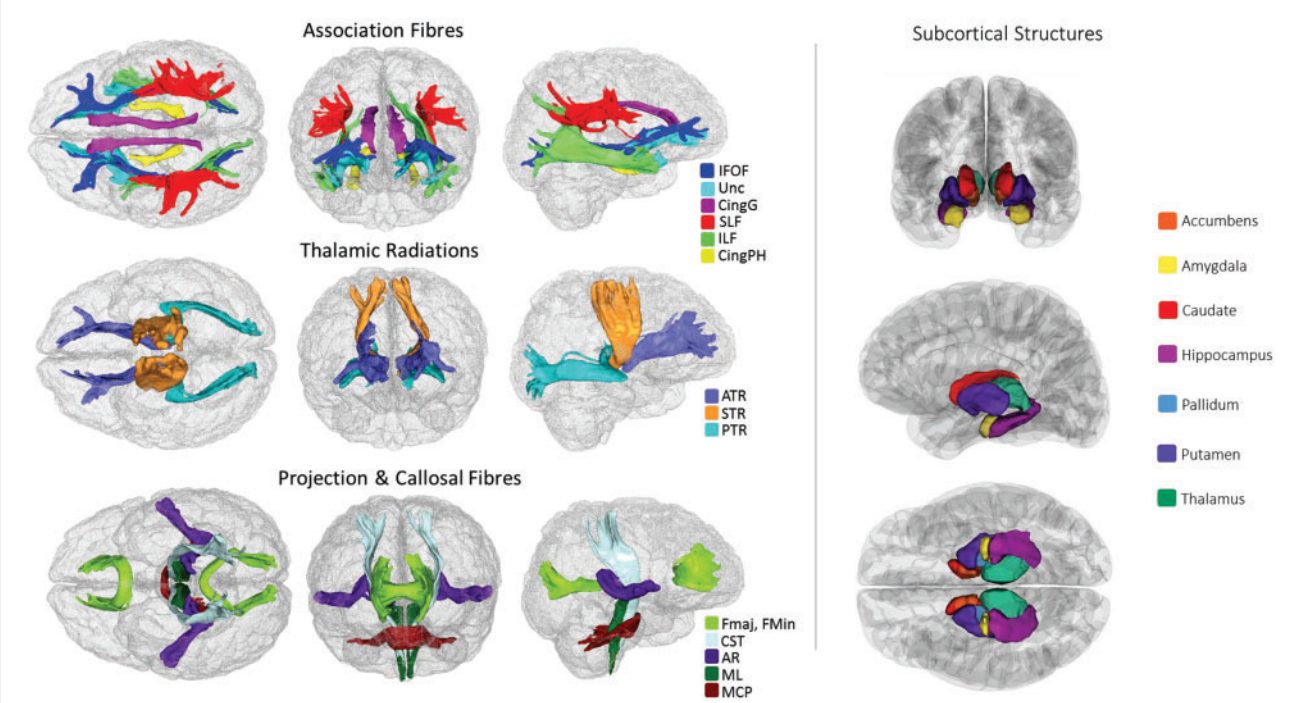

Figure 1 White matter tracts-of-interest (left panel) and subcortical structures (right panel) measured in the current study. AR, acoustic radiation; ATR, anterior thalamic radiation; Cing, cingulum (gyrus and parahippocampal); CST, corticospinal tract; Fmaj and Fmin (forceps major and minor); IFOF, inferior fronto-occipital fasciculus; ILF, inferior longitudinal fasciculus; MCP, middle cerebellar peduncle; ML, medial lemniscus; PTR, posterior thalamic radiation; SLF, superior longitudinal fasciculus; STR, superior thalamic radiation; Unc, uncinate fasciculus.

In addition to UK Biobank-provided IDPs, we conducted local processing and QC of cortical reconstruction and segmentation, using FreeSurfer v5.3 on T_1-weighted volumes. Following visual inspection of the outputs (to check for aberrant surfaces and tissue segmentation failures, which were removed from analysis), a total of 8975 participants had cortical surfaces available for analysis, 7928 of whom also had casewise complete vascular, demographic and covariate data, and were used in the vertex-wise analyses. Surfaces were aligned vertex-wise into common space (the Freesurfer average template) and smoothed at 20 mm full width at half maximum, allowing sample-wide analyses of volume across the cortical mantle.

Analyses

All variables were visually inspected to ascertain whether they were distributed normally. BMI and WMH were log-transformed to correct a positively skewed distribution. We subsequently refer to total brain volume corrected for head size as global atrophy. The ethnicity of the group was predominantly white, with 203 participants categorizing themselves as non-white; this dichotomous variable for ethnicity was used as a covariate in all analyses. Pack years was calculated as the number of cigarettes per day divided by 20, and then multiplied by the number of years participants reported having smoked for. A latent measure of general white matter fractional anisotropy (*g*FA) and mean diffusivity (*g*MD) were derived using confirmatory factor analysis ('cfa' in the lavaan package) to index the high degree of covariance among white matter microstructural properties across the brain, as previously reported in this cohort[28] and in others.[29,30]. As described previously,[28] all tract measures (left and right) were entered separately into this analysis, correlated residuals between the left and right of each tract and between some other tracts were allowed, and based on low loadings (<0.3) of the Medial Lemniscus, Middle Cerebellar Peduncle and bilateral Parahippocampal Cingulum on the first factor, these measures were not included in the factor analysis. Tract loadings and model fit are shown in Supplementary material online, *Table S1*.

We used two methods to capture the overall VRF load per individual. First, we derived an aggregate measure of vascular risk for each individual, counting instances of a self-reported diagnosis of hypertension, diabetes, or hypercholesterolaemia, having ever smoked, having a BMI >25,[31,32] and having a high WHR (>0.85 for females and >0.90 for males[33]). We also derived a latent factor of general vascular risk (*g*VRF) following prior work in an older cohort, using confirmatory factor analysis in structural equation modelling.[34] This latent measure captures, and depends upon, the tendency for VRFs to co-occur. Using 'cfa' from the lavaan package, *g*VRF was derived from smoking pack years, diastolic and systolic blood pressure, BMI, WHR, self-reported hypertension, diabetes and hypercholesterolaemia. The model fit the data well, though loadings were inconsistent (range 0.175–0.758), with the factor more strongly loaded towards BMI and WHR (see Supplementary material online, *Table S2*).

First, we conducted descriptive analyses, testing associations between age and sex with each VRF (pack years, hypertension, pulse pressure, diabetes, hypercholesterolaemia, BMI, and WHR) using linear regression (except for binary VRFs where logistic regression was used). We then examined associations between global MRI measures (total brain volume, grey matter volume, WMH, *g*FA, and *g*MD) and overall and individual VRFs. To illustrate the real-terms implications, we conducted a propensity score matching analysis. Individuals with a total of five or six VRFs were each matched on sex, age, and head size to a single participant who had no VRFs. We used 'ps.match' in the 'non-random' package with a logit

calliper width of 0.05. To optimize group matching, participants were manually split by sex for matching, and then recombined, after which the groups were compared on raw volumetric brain indices.

We then tested associations at the regional MRI level. We ran linear regression analyses to quantify associations between overall load of VRFs (aggregate and latent VRF variables) and global MRI indices. We also included all age × VRF interactions; a significant interaction would mean that there was a difference association magnitude at different ages. In order to adequately correct our interaction term for the effects of sex, age, and age^2 (i.e. non-linear), we also included sex × age and sex × age^2 as covariate terms.[35,36] We also covaried for ethnicity, head size, and differences in head positioning inside the scanner (X, Y, and Z co-ordinates; http://biobank.ctsu.ox.ac.uk/showcase/label.cgi?id=110), which were mean centred.

Next, we examined associations between each individual VRF and global MRI measures. Initially, we ran a separate simple model in which one VRF predicted each global MRI measure in turn, corrected for age, sex, ethnicity, head size, and scanner head position. We then re-ran these models to include a VRF × age interaction term, as described above. Finally, accounting for the fact that VRFs are positively correlated, we examined the unique contributions of each VRF to global brain MRI measures by including all VRFs in one multiple linear regression for each MRI variable of interest. This approach allowed us to parse the relative contributions of each VRF—in the context of all others—to variance in brain MRI variables. To quantify the amount of variance in each brain imaging biomarker accounted for by VRFs, we compared the R^2 of each model with that from a baseline model R^2 in which the MRI measure was modelled with covariates only.

We then examined associations between regional MRI measures (white matter tract-specific FA and MD, vertex-wise cortical volume, and subcortical volumes) and the latent and aggregate measures of vascular risk. Finally, we examined the associations between individual VRFs and regional brain MRI. To do this, we first showed the basic associations for each individually modelled VRF, before fitting a multiple regression for each of these regional MRI measures in which all individual VRFs were entered together. As before, all models also included age, sex, ethnicity, head size (for volumetric data), and head positioning confounds.

Statistical analyses were performed in R version 3.5.0 (https://www.r-project.org) except for cortical surface analyses which were performed using the SurfStat MATLAB toolbox (http://www.math.mcgill.ca/keith/surfstat) for Matrix Laboratory R2012a (The MathWorks, Inc., Natick, MA, USA). We ensured that models showed acceptably low multicollinearity (variance inflation was ascertained using 'vif' in the 'car' package in R). Alpha was set at 0.05 for all analyses and results were corrected for multiple comparisons using the false discovery rate (FDR)[37] using 'p.adjust' function in the 'stats' package in R. Standardized coefficients are reported throughout to facilitate comparison of associations across all VRFs. The magnitude of effects can be classified according to Cohen,[38] whereby the effect sizes are small, medium, or large when the standardized coefficients are 0.1, 0.3, or 0.5, respectively. Maps of the *t*-statistics for cortical analyses were displayed on the mantle such that negative associations with a VRF (i.e. lower volume) were always represented by the red end of the colour spectrum.

Results

Participants were aged between 44.23 and 79.41 ($M = 61.97$, SD = 7.48) years, and participant characteristics are shown in *Table 1*. When modelling each VRF on age, sex, and age × sex (see Supplementary material online, *Table S3*), males had significantly higher levels on all risk factors, and there were significant age × sex interactions for pack years ($\beta = 0.039$), pulse pressure ($\beta = -0.049$), and aggregate vascular risk ($\beta = 0.025$). There was a significant association between greater vascular risk and older age across all VRFs (β range 0.083–0.498) except for BMI which showed a weak relationship in the opposite direction (β = -0.027). Plots of simple VRF trends with age are presented in Supplementary material online, *Figure S1*. Consistent with the full UK Biobank cohort,[39] VRFs were generally modestly but significantly correlated (see Supplementary material online, *Figure S2* and *Table S4*). Older age was a relatively strong predictor of greater global atrophy and WMH volume, lower grey matter volume and gFA, and higher gMD (see Supplementary material online, *Table S4*; β range |0.254| to |0.586|), consistent with prior reports from the initial release of UK Biobank MRI data (N ≈ 5000[28,40]). Sex differences in brain MRI measures were consistent with those previously described in a smaller UK Biobank sample.[41]

Global brain MRI analyses

General vascular risk

Associations between aggregate vascular risk and global MRI measures are reported in *Table 2*. Having a larger number of VRFs was associated with ostensibly 'poorer' global brain MRI health across all measures (β range |0.042| to |0.110|), accounting for ~1% of the variance in brain MRI measures beyond the contribution of covariates. Aside from the modest but significant positive interaction between age and aggregate VRF on higher gMD (interaction $\beta = 0.036$; main effect $\beta = 0.072$; indicating more VRFs are more strongly associated with less healthy white matter in older age), there was no evidence that associations between global brain measures and general vascular risk were stronger at different ages.

The propensity score matching procedure yielded two groups of 235 individuals who were matched on age, sex, and head size (see Supplementary material online, *Table S5*). On average, when compared with individuals with no VRFs, individuals with five or six VRFs had 17 927 mm^3 (1.5%) lower brain volume, 17 869 mm^3 (2.89%) less total grey matter, and 1191 mm^3 (51.54%) greater WHM burden.

Alongside a measure of aggregate vascular risk, we quantified a latent factor of vascular risk (gVRF[34]), which showed a good fit to the data (see Supplementary material online, *Figure S2* and *Table S2*). The measure of aggregate VRF and gVRF were strongly correlated ($r = 0.795$). Whereas gVRF exhibited numerically larger association magnitudes with all global MRI measures apart from MD (see Supplementary material online, *Table S6*), these differences were modest; however, owing to the large N in the present study, we could detect that the gVRF associations were significantly larger for grey matter volume [$t(9719) = 3.401$, $P < 0.001$] and WMH volume [$t(8859) = 2.222$, $P = 0.026$].

Individual vascular risk factors

Associations between global brain MRI measures and individual VRFs are also reported in *Table 2*. A greater number of pack years smoked, and a diagnosis of hypertension or diabetes were independently associated with putatively poorer global brain structural parameters (greater global atrophy, lower grey matter volume, more WMH, lower gFA, and higher gMD; β range |0.022| to |0.104|). Higher BMI and WHR were both consistently associated with greater global

Table 1 Participant characteristics

Variable	Units	Descriptor	N
Demographics			
Age	Years *M* (SD)	61.97 (7.48)	9722
Sex	F (%F)	5105 (52.51)	9722
Ethnicity	White British (%)	9519 (98)	9722
VRFs			
Smoker[a,m]	Current:Ex:Never	399:3322:5910	9631
Pack years	Years *M* (SD)	4.76 (11.11)	9631
Hypertension[a,m]	Yes (Yes%)	2002 (20.59)	9722
Pulse pressure[a,m]	mm Hg *M* (SD)	57.03 (13.39)	9346
Diabetes[a,m]	Yes (Yes%)	476 (5.90)	9722
Hypercholesterolaemia[a,m]	Yes (Yes%)	1069 (11.00)	9722
BMI[a,m]	Kg/m^2 median (IQR)	26.08 (5.36)	9693
WHR[a,m]	W:H *M* (SD)	0.86 (0.08)	9695
Brain MRI			
Total brain volume	mm^3 *M* (SD)	1 166 776 (110 729.90)	9722
Grey matter volume	mm^3 *M* (SD)	615 142.30 (55 039.46)	9722
WMH volume	mm^3 median (IQR)	2147.00 (3007.00)	8861
gFA	Std units *M* (SD)	0 (1)	8601
gMD	Std units *M* (SD)	0 (1)	8514

Heart or cardiac problem includes self-report of angina. Brain MRI volumes are raw values (uncorrected for head size). Significant positive association between greater vascular risk and [a]age, and [m/f]gender (see Supplementary material online, *Table S3*).
BMI, body mass index; VRF, vascular risk factor; WHR, waist–hip ratio; WMH, white matter hyperintensity, *g*FA and *g*MD (latent factors of white matter fractional anisotropy and mean diffusivity).

atrophy, lower grey matter volume and higher WMH load, but both were non-significant for *g*FA, and only WHR was associated with higher *g*MD. Higher pulse pressure was associated with poorer white matter measures (higher WMH and MD, and lower FA), but was also related to less global atrophy ($\beta = 0.24$). Finally, a diagnosis of hypercholesterolaemia was only significantly associated with greater WMH load, but with no other MRI index. No significant interactions were found between individual VRFs and global brain measures (see Supplementary material online, *Table S7*), and so age × VRF interactions were not further investigated at the brain regional level.

Simultaneous modelling of individual VRF-global brain associations indicated that the contributions of VRFs were mostly independent. Overall, magnitudes of associations between VRFs and global MRI variables were modest, explaining a small amount of additional variance beyond covariates. In order of smallest to largest, the incremental R^2 explained by all VRFs was: global atrophy = 0.004, *g*FA = 0.011, grey matter volume = 0.011, *g*MD = 0.015, WMH = 0.018 (*Table 2*). The numerically largest associations were for hypertension on white matter measures (β range |0.080| to |0.094|), whereas self-reported hypercholesterolaemia did not make any significant unique contribution—above other VRFs—to any global MRI measure ($\beta \leq 0.007$). The most notable effect of simultaneously modelling VRFs was that, whereas WHR still showed significant associations with global volumetric MRI measures (global atrophy, grey matter volume, and WMH volume), the magnitude was attenuated by ∼50%, and BMI was no longer significantly associated with any MRI measure except grey matter volume. This, however, indicates that variance in both BMI and WHR made unique contributions to lower grey matter volumes. Pack years, hypertension, pulse pressure, and diabetes were still most consistently linked across all global brain outcomes.

Regional brain MRI analyses

General vascular risk

We tested whether there was regional specificity underlying the global MRI associations between general and specific vascular risk. Vertex-wise cortical analysis revealed widespread significant associations between higher aggregate vascular risk and lower cortical volume (*Figure 2*). The FDR-corrected *q*-map illustrates the comparative sparing of dorsal motor/somatosensory and posterior cortical regions, while the t-map indicates largest effect sizes in the frontal and especially anterior lateral and medial temporal lobes.

Results of the associations of aggregate vascular risk with white matter tract FA and MD, and with subcortical volumes are shown in *Figure 2* and Supplementary material online, *Table S8*. Higher aggregate vascular risk was associated with lower FA and higher MD and particularly implicated association and thalamic fibres. Unexpectedly, we also found some associations with projection fibres which were numerically among the largest magnitudes but in the opposite direction; higher aggregate risk was associated with *higher* FA in the corticospinal tract ($\beta = 0.052$), and middle cerebellar peduncle ($\beta = 0.065$), and also with *lower* MD in the medial lemniscus ($\beta = -0.060$). Higher aggregate vascular risk was also associated with generally lower subcortical volumes in all structures (β range -0.087 to -0.046) except the amygdala ($\beta = -0.006$).

Table 2 Associations between individually and simultaneously modelled vascular risk factors on global brain MRI parameters

Vascular		Global atrophy		GM		WMH		gFA		gMD	
risk factors	Model	*β*	*P*	*B*	*P*	*β*	*P*	*β*	*P*	*β*	*P*
Aggregate VRF	–	**−0.061**	**<0.001**	**−0.097**	**<0.001**	**0.110**	**<0.001**	**−0.042**	**<0.001**	**0.072**	**<0.001**
× Age	–	0.005	0.607	-0.002	0.785	-0.014	0.163	-0.019	0.093	**0.036**	**<0.001**
Additional R^2		0.005		0.008		0.010		0.002		0.007	
Total R^2		0.344		0.474		0.321		0.099		0.184	
Pack years	Single	**−0.037**	**<0.001**	**−0.061**	**<0.001**	**0.076**	**<0.001**	**−0.036**	**<0.001**	**0.044**	**<0.001**
	Simultaneous	**−0.029**	**<0.001**	**−0.046**	**<0.001**	**0.062**	**<0.001**	**−0.033**	**0.002**	**0.036**	**<0.001**
Hypertension	Single	**−0.027**	**0.001**	**−0.037**	**<0.001**	**0.097**	**<0.001**	**−0.084**	**<0.001**	**0.104**	**<0.001**
	Simultaneous	**−0.022**	**0.012**	**−0.022**	**0.006**	**0.080**	**<0.001**	**−0.084**	**<0.001**	**0.094**	**<0.001**
Pulse pressure	Single	**0.024**	**0.008**	0.013	0.122	**0.069**	**<0.001**	**−0.044**	**<0.001**	**0.074**	**<0.001**
	Simultaneous	**0.033**	**<0.001**	**0.024**	**0.004**	**0.053**	**<0.001**	**−0.033**	**0.005**	**0.058**	**<0.001**
Diabetes	Single	**−0.044**	**<0.001**	**−0.066**	**<0.001**	**0.065**	**<0.001**	-0.037	**<0.001**	**0.045**	**<0.001**
	Simultaneous	**−0.037**	**<0.001**	**−0.050**	**<0.001**	**0.038**	**<0.001**	-0.022	0.041	**0.028**	**0.007**
High cholesterol	Single	-0.003	0.712	-0.006	0.434	**0.023**	**0.009**	-0.007	0.520	0.016	0.099
	Simultaneous	0.007	0.402	0.001	0.200	0.003	0.788	0.004	0.693	0.001	0.909
BMI	Single	**−0.037**	**<0.001**	**−0.078**	**<0.001**	**0.053**	**<0.001**	0.003	0.749	0.013	0.209
	Simultaneous	-0.012	0.240	**−0.043**	**<0.001**	0.003	0.790	0.026	0.041	-0.028	0.022
WHR	Single	**−0.060**	**<0.001**	**−0.101**	**<0.001**	**0.082**	**<0.001**	-0.000	0.981	**0.041**	**0.002**
	Simultaneous	**−0.036**	**0.007**	**−0.050**	**<0.001**	**0.048**	**<0.001**	0.007	0.685	0.027	0.086
VRF added R^2		0.004		0.011		0.018		0.011		0.015	
Total R^2		0.343		0.476		0.325		0.106		0.185	

Standardized betas (β) and *P*-values are reported from regression models where VRFs are regressed onto MRI measures, covarying for ethnicity, sex, age, sex × age, and head position MRI confounds (volumetric data are also corrected for head size). Model denotes the results for each VRF modelled individually, and then when modelled simultaneously alongside all other VRFs. Additional R^2 refers to the amount of variance in MRI measures accounted for by the simultaneously modelled VRFs, beyond covariates. Bold text denotes FDR *q*-value <0.05.

BMI, body mass index; GM, grey matter volume; VRF, vascular risk factor; WHR, waist–hip ratio; WMH, white matter hyperintensity, *g*FA and *g*MD (latent factors of white matter fractional anisotropy and mean diffusivity).

The corresponding analysis for *g*VRF showed an almost identical pattern for cortical, white matter and subcortical measures (see Supplementary material online, *Figure S3* and *Table S9*), though association magnitudes were, on average, slightly stronger throughout. For the vertex-wise analysis, this resulted in slightly higher *t*-values which were significant across slightly less restricted cortical loci, and was also the case for subcortical values.

Individual vascular risk factors

The patterning of significant associations of each individually modelled VRF across the brain's cortex are shown in *Figure 3*. All FDR-corrected (*q*) significant associations were in the expected direction (higher VRF with lower volume). Pulse pressure and hypercholesterolaemia showed no FDR-corrected significant associations with the cortex (see Supplementary material online, *Figure S4*). For pack years, hypertension, diabetes, BMI, and WHR, a consistent pattern of associations emerged where the strongest effects in each case were in the lateral and medial temporal lobes. As with overall vascular risk, cortical associations towards the vertex were consistently absent. Medial and lateral frontal areas also showed significant associations, and relationships with occipital regions were most evident for smoking and diabetes.

Simultaneous modelling of individual VRFs across the cortex revealed the extent to which each VRF made a unique contribution to variance in regional volume, accounting for all other VRFs (see Supplementary material online, *Figure S5*). Though effect sizes were generally weaker, and the FDR-corrected loci were more restricted than when individually modelled, the patterning of associations was largely unaltered. The common and unique patterns were more formally compared in the conjunction and conditional cortical analyses (see Supplementary material online, *Figure S6*). This emphasizes clearly that (i) individual VRFs make unique contributions to lower cortical volume at specific—common—foci: medial and anterior frontal, and temporal cortex, and (ii) there were also regions which showed no overlap, indicating VRF-specific associations.

Associations between individually modelled VRFs and white matter tract microstructure are reported in *Figure 4* and Supplementary material online, *Tables S10 and S11*. Thalamic and association fibres and the forceps minor showed the most consistent associations with lower FA and higher MD. These were driven by hypertension, pulse pressure, diabetes, and pack years (β range |0.023| to |0.106|), in contrast to BMI and WHR whose associations were more consistent across projection bundles. Hypercholesterolaemia was not significantly associated with FA or MD in any tract.

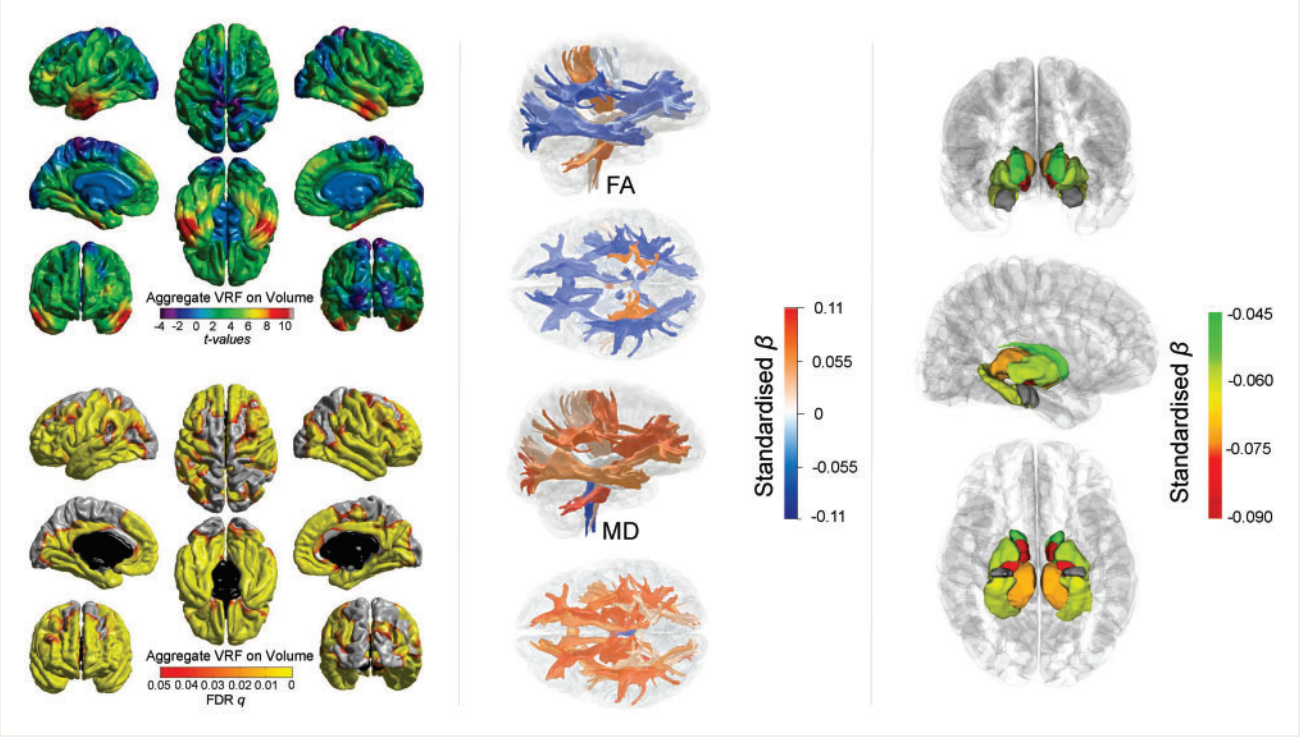

Figure 2 Associations between aggregate vascular risk and cortical volume (left panel), white matter tract-specific microstructure (centre panel showing right lateral and superior views), and subcortical volume (right panel showing, from top to bottom: anterior, lateral, and inferior views). Higher aggregate vascular risk is associated with significantly lower cortical volume, lower fractional anisotropy and higher mean diffusivity in the majority of white matter fibres, and lower subcortical volume, except for the amygdala (grey).

Associations between subcortical volumes and VRFs are reported in *Figure 4* and Supplementary material online, *Table S12*. The majority of VRFs were significantly associated with lower volumes of all subcortical structures (β range |0.024| to |0.085|) except for the amygdala. However, hypercholesterolaemia was only associated with lower accumbens (β = -0.028) and thalamus volumes (β = -0.019), and pulse pressure showed no significant associations at all. Simultaneously modelling all VRFs for each tract (see Supplementary material online, *Tables S13* and *S14*) and subcortical volume (see Supplementary material online, *Table S15*) did not substantially change this pattern of results, suggesting that effects are mainly independent from each other. However, high cholesterol was no longer significantly related to any subcortical volume.

Discussion

Interpretation

In this large, single-scanner sample of middle- and older-aged adults, associations between greater vascular risk and poorer brain health were small but significant across cortical, white matter, and subcortical tissue; there was a dose effect whereby the magnitude of association increased with the number of VRFs. Notably, individuals with the highest levels of VRF burden had, on average, 50% greater WMH burden than those with no VRFs who were matched on age, sex, and head size (though there was considerable group overlap). Associations between vascular risk and brain structure did not differ appreciably across the sampled age range. We also provide insight into the relative contributions of different VRFs to brain health: greater pack years, a diagnosis of hypertension and diabetes each made unique contributions to poorer brain health across grey matter and WMH volume, white matter microstructure, and subcortical volume. Conversely, pulse pressure was mainly related to white but not grey matter measures, whereas WHR was only uniquely associated with volumetric grey and WMH (but not microstructure). A diagnosis of hypercholesterolaemia made no unique contributions to brain health beyond other risk factors.

Throughout, effect sizes were mainly small according to Cohen,[38] accounting for less than 2% of the variance in brain structure. By providing very accurate estimates of effect sizes in this very large sample, we provide guidance to researchers and clinicians on the range of effects to plausibly expect in designing future studies and interventions. The presence of significant associations between vascular factors and brain health in this relatively healthy sample (which was of the same magnitude, irrespective of age) has implications for the potential for the management of malleable VRFs—among those of comparatively good health, and even in middle age—to improve and brain and cognitive ageing.

Our results provide further evidence for regional cerebral vulnerability to VRFs in healthy individuals. On the cortex, associations between aggregate vascular risk and lower cortical volume shows

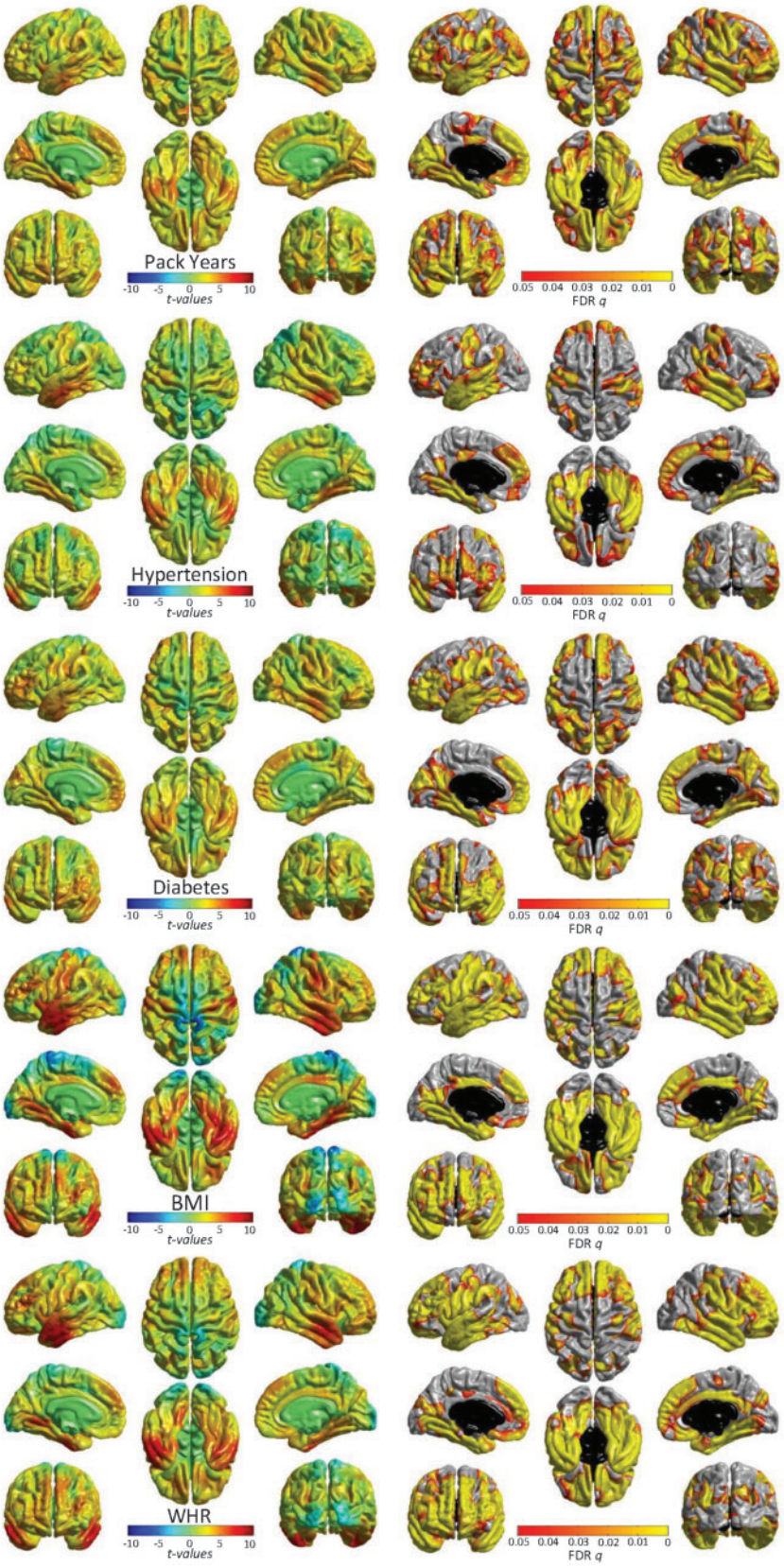

Figure 3 Significant associations (left: *t*-maps and right: FDR-corrected *q*-values) between cortical volume and vascular risk factors (modelled individually, alongside age, sex, ethnicity, head size, and scanner head position confounds). See Supplementary material online, *Figure S3* for non-significant associations for pulse pressure and hypercholesterolaemia. T-maps are scaled with the same limits to aid comparison of relative effect size across risk factors.

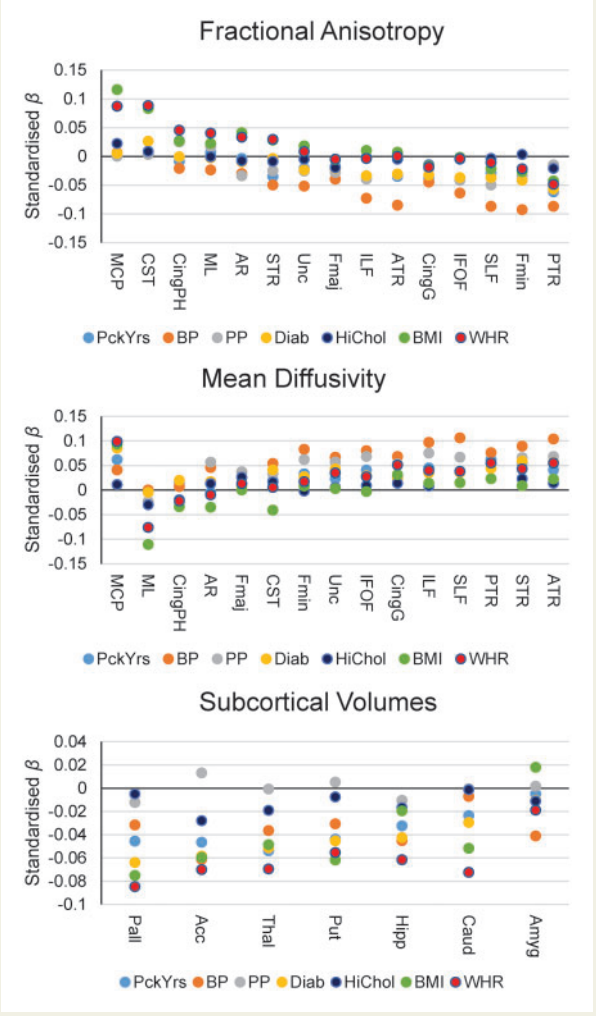

Figure 4 Standardized betas of associations between individually modelled vascular risk factors and white matter tract fractional anisotropy (top panel), white matter tract mean diffusivity (centre panel), and subcortical volumes (bottom panel). Acc, accumbens; Amyg, amygdala; ATR, anterior thalamic radiation; BP, hypertension; Caud, caudate; Cing, cingulum (gyrus and parahippocampal); CST, corticospinal tract; Diab, diabetes; Fmaj and Fmin (forceps major and minor); HiChol, hypercholesterolaemia. AR, acoustic radiation; Hipp, hippocampus; IFOF, inferior fronto-occipital fasciculus; ILF, inferior longitudinal fasciculus; MCP, middle cerebellar peduncle; ML, medial lemniscus; Pall, pallidum; PP, pulse pressure; PTR, posterior thalamic radiation; Put, putamen; SLF, superior longitudinal fasciculus; STR, superior thalamic radiation; Thal, thalamus; Unc, uncinate fasciculus.

strongest effects on frontal and especially anterior lateral and medial temporal lobes, rather than dorsal motor/somatosensory and posterior cortical regions. The cortical patterning in this large healthy sample is more extensive than the areas associated with cardiac regulation,[20,21] agrees with loci associated with other markers of CSVD in community-dwelling adults,[42,43] and is strikingly consistent with the regional ischaemic vulnerability of the brain to hypoperfusion in clinical samples[44] and the pattern of atrophy common in 'typical' Alzheimer's disease.[45]

We find that greater vascular risk is related to 'poorer' white matter microstructure (higher MD and lower FA) in specific classes of white matter tract. The association and thalamic radiations along with the forceps minor showed the most consistent significant relationships with vascular risk. These pathways also appear most susceptible to ageing, and we had previously hypothesized that this susceptibility and the phenomenon of age-related (statistical) de-differentiation might be partly driven by the disproportionately negative effects of environmental factors on these same fibres.[28] This also concurs with an explanation that these fibres connect the most metabolically active regions of the brain[46] and may be at greatest risk of neurovascular ageing.[15,19,44] Finally, higher vascular risk was related to modestly lower subcortical volumes across the accumbens, caudate, hippocampus, pallidum, putamen, and thalamus. Subcortical atrophy and WMH burden are also related to clinical diagnoses of dementia and vascular cognitive impairment.[47]

As far as we are aware, this is the largest single-scanner study of multiple VRFs and multi-modal structural brain imaging to-date. The high statistical power allowed us to reliably detect subtle and non-overlapping contributions of multiple individual VRFs to a large variety of brain health markers. Though there is some tendency for VRFs to co-occur, our simultaneous modelling indicated that smoking, hypertension, pulse pressure, diabetes, and WHR each made unique statistical contributions to lower global brain and higher WMH volumes. Whereas it is possible that associations between obesity and brain structure are partly attributable to the findings that obesity promotes arterial stiffness, it is possible that the unique statistical contributions identified herein could pertain to other mechanisms through which body composition is linked to negative brain and cognitive endpoints, including metabolic and endocrine routes, which may have independent neurovascular consequences.[17,26,48] Similarly, the unique contributions to brain structure made by hypertension and smoking may indicate that the deleterious effects of smoking on the brain extend beyond putative alterations in hypertension.[49] This adds to the literature on the complex interplay between multiple sources of vascular risk and their associations with brain health.

Limitations

The age range does not cover older ages (upper age limit was 79 years), restricting the degree to which our findings can be generalized to other populations. This may also have limited our scope to identify age–VRF interactions; such effects may be driven by very small associations in individuals who are much older than participants included here.[25] The UK Biobank imaging sample shows a tendency to live in less deprived areas than other UK Biobank participants,[50] who are already range restricted compared with the general population,[51] which may limit generalizability. Nevertheless, it is striking that associations between VRFs and brain structure are detectable even in these relatively healthy individuals, and effects may be larger in a more population-representative sample. These data are cross-sectional, and cannot speak to lifelong trends in vascular risk, trajectories of brain regional decline nor important aspects such as lead-lag effects. Though we made attempts to remove individuals with neurological or neurodegenerative disorders, it is not possible to ascertain the degree to which the results reported here are driven by individuals with nascent age-related clinical neurodegenerative conditions.

However, the lack of VRF × age interactions might militate against a substantial confound.

The VRFs themselves represent different levels of fidelity—hypertension, diabetes, and hypercholesterolaemia were binary rather than continuous measures, and all were based on self-report (albeit via a medical interview with a nurse). As a consequence, it is possible that individual variability on continuous measures (such as blood cholesterol, or HbA1c) would prove more informative for brain outcomes. However, this alone cannot explain the null hypercholesterolaemia associations, given the results for diabetes and hypertension. Though the simultaneous modelling of individual VRFs did not fundamentally alter the pattern of simple main effect, the combination of dichotomous and continuous variables could mean that any attenuations of estimates (from individual models) could partly be driven by this limitation, and should be interpreted with appropriate caution. On a related note, efficacy, dosage, and time since diagnosis are all pertinent factors not measured here. These and other vascular risk markers may well interact with differences in genetic susceptibility to determine brain and cognitive outcomes (e.g.[52,53]), and is a priority for future study.

Whereas the imaging acquisition and variety of sequences acquired can be considered state-of-the-art, the limitations of dMRI, and of assuming that higher FA and lower MD automatically relate to 'poorer' white matter microstructure or health, should be observed. There are many microstructural (including myelination, axonal bore, crossing fibres) and methodological factors that influence measurement of water molecular diffusion, necessitating a more nuanced interpretation.[54] This is evident in the conflicting directions of association between projection fibres compared with callosal, thalamic, and association tracts. Taking the example of the middle cerebellar peduncle (which showed positive FA and MD betas)—in complex fibre structures with multiple crossing pathways, one can envisage a situation where FA and MD are positively correlated when more degraded transecting fibres provide less interference to molecular diffusion along the principal direction of the tract, thus leading to increases in both the directional coherence and the overall magnitude of water molecular diffusion.

Summary

Elevated vascular risk in this large group of community-dwelling adults from the general population was related to poorer brain health. A larger accumulation of VRFs increased the magnitude of the association. The patterning of these effects was most pronounced in areas linked to elevated stroke and hypoperfusion susceptibility, and typical Alzheimer's disease atrophy, and in the white matter pathways that facilitate their connectivity. Smoking, diabetes, and hypertension showed the most consistent associations across global and regional brain measures.

Supplementary material

Supplementary material is available at *European Heart Journal* online.

Acknowledgements

We thank the UK Biobank participants and the UK Biobank team for their work in collecting, processing, and disseminating these data for analysis. This research was conducted, using the UK Biobank Resource under approved project 10279, in The University of Edinburgh Centre for Cognitive Ageing and Cognitive Epidemiology (CCACE; http://www.ccace.ed.ac.uk), part of the cross-council Lifelong Health and Wellbeing Initiative (MR/K026992/1).

Funding

Funding from the Biotechnology and Biological Sciences Research Council (BBSRC) and Medical Research Council (MRC) is gratefully acknowledged. S.R.C., M.E.B., J.M.W., and I.J.D. were supported by MRC grants MR/M013111/1 and MR/R024065/1. I.J.D. is additionally supported by the Dementias Platform UK (MR/L015382/1), and he, S.R.C., S.J.R., M.E.B. and J.M.W. by the Age UK-funded Disconnected Mind project (http://www.disconnectedmind.ed.ac.uk). J.M.W. is supported by the Fondation Leducq Transatlantic Network of Excellence, ref no. 16 CVD 05. S.R.C., S.J.R., C.R.B., M.E.B., I.J.D., and E.M.T.-D. were supported by a National Institutes of Health (NIH) research grant R01AG054628. E.M.T.-D. was also supported by National Institutes of Health (NIH) research grant RO1HD083613. E.M.T.-D. is a member of the Population Research Center at the University of Texas at Austin, which is supported by NIH centre grant P2CHD042849. J.M.W. was supported by the Scottish Imaging Network: A Platform for Scientific Excellence (SINAPSE) collaboration (http://www.sinapse.ac.uk). C.F.-R. is supported by Dementias Platform UK (DPUK), funded through the MRC (MR/L023784/2).

Conflict of interest: none declared.

References

1. Academy of Medical Sciences. Influencing the trajectories of ageing; 2016. https://tinyurl.com/acadmedsci2016 (30 November 2018).
2. House of Lords. *Ageing: Scientific Aspects*. London: The Stationery Office; 2005.
3. Kirkwood T. *Foresight Mental Capital and Wellbeing Project 2008: Final Project Report Executive Summary. Mental Capital through Life*. London: Government Office for Science; 2008.
4. Jekel K, Damian N, Wattmo C, Hausner L, Bullock R, Connelly PJ, Dubois PJ, Eriksdotter M, Ewers M, Graessel E, Kramberger MG, Law E, Mecocci P, Molinuevo JL, Nygard L, Olde-Rikkert MG, Orgogozo JM, Pasquier F, Peres K, Salmon E, Sikkes SA, Sobow T, Spiegel R, Tsolaki M, Winblad B, Frolich L. Mild cognitive impairment and deficits in instrumental activities of daily living: a systematic review. *Alzheimers Res Ther* 2015;**7**:17.
5. Tucker-Drob EM. Neurocognitive functions and everyday functions change together in old age. *Neuropsychology* 2011;**25**:368–377.
6. Boyle PA, Yu L, Wilson RS, Gamble K, Buchman AS, Bennett DA. Poor decision making is a consequence of cognitive decline among older persons without Alzheimer's disease or mild cognitive impairment. *PLoS One* 2012;**7**:e43647.
7. Fineberg NA, Haddad PM, Carpenter L, Gannon B, Sharpe R, Young AH, Joyce E, Rowe J, Wellsted D, Nutt DJ, Sahakian BJ. The size, burden and cost of disorders of the brain in the UK. *J Psychopharmacol* 2013;**27**:761–770.
8. Wimo A, Jonsson L, Bond J, Prince M, Winblad B, Alzheimer DI. The worldwide economic impact of dementia 2010. *Alzheimers Dement* 2013;**9**:1–11.e3.
9. Plassman BL, Langa JM, Fisher GG, Heeringa SG, Weir DR, Ofstedal MD, Burke JR, Hurd MD, Potter GG, Rodgers WL, Steffens DC, McArdle JJ, Willis RJ, Wallace RB. Prevalence of cognitive impairment without dementia in the United States. *Ann Intern Med* 2008;**148**:427–434.
10. Bárrios H, Narciso S, Guerreiro M, Maroco J, Logsdon R, de Mendonca A. Quality of life in patients with mild cognitive impairment. *Aging Ment Health* 2013;**17**:289–292.
11. Lyall DM, Celis-Morales CA, Anderson J, Gill JMR, Mackay DF, McIntosh AM, Smith DJ, Deary IJ, Sattar N, Pell JP. Associations between single and multiple cardiometabolic diseases and cognitive abilities in 474 129 UK Biobank participants. *Eur Heart J* 2016;**38**:577–583.
12. Samieri C, Perier M-C, Gaye B, Proust-Lima C, Helmer C, Dartigues J-F, Berr C, Tzourio C, Empana J-P. Association of cardiovascular health level in older age with cognitive decline and incident dementia. *JAMA* 2018;**320**:657–664.
13. Shi Y, Wardlaw JM. Update of cerebral small vessel disease: a dynamic whole-brain disease. *Stroke Vasc Neurol* 2016;**25**:83–92.
14. Pantoni L. Cerebral small vessel disease: from pathogenesis and clinical characteristics to therapeutic challenges. *Lancet Neurol* 2010;**9**:689–701.

15. de la Torre JC. Cerebral hemodynamics and vascular risk factors: setting the stage for Alzheimer's disease. *J Alzheimers Dis* 2012;**32**:553–567.
16. Pasha EP, Birdsill AC, Oleson S, Haley AP, Tanaka H. Impacts of metabolic syndrome scores on cerebrovascular conductance are mediated by arterial stiffening. *Am J Hypertens* 2018;**31**:72–79.
17. Haley AP, Oleson S, Pasha E, Birdsill A, Kaur S, Thompson J, Tanaka H. Phenotypic heterogeneity of obesity-related brain vulnerability: one-size interventions will not fit all. *Ann N Y Acad Sci* 2018;**1428**:89–102.
18. Sweeney MD, Kisler K, Montagne A, Toga AW, Zlokovic BV. The role of brain vasculature in neurodegenerative disorders. *Nat Neurosci* 2018;**21**:1318–1331.
19. Mitchell GF, van Buchem MA, Sigurdsson S, Gotal JD, Jonsdottir MK, Kjartansson Ó, Garcia M, Aspelund T, Harris TB, Gudnason V, Launer LJ. Arterial stiffness, pressure and flow pulsatility and brain structure and function: the age, gene/environment susceptibility—Reykjavik study. *Brain* 2011;**134**:3398–3407.
20. Klein C, Hiestand T, Ghadri JR, Templin C, Jänke L, Hänggi J. Takotsubo syndrome – predictable from brain imaging data. *Sci Rep* 2017;**7**:5434.
21. Hiestand T, Hänggi J, Klein C, Topka MS, Jaguszewski M, Ghadri JR, Lüscher TF, Jäncke L, Templin C. Tokotsubo syndrome associated with structural brain alterations of the limbic system. *J Am Coll Cardiol* 2018;**71**:809–811.
22. Mosconi L, Walters M, Sterling J, Quinn C, McHugh P, Andrews RE, Matthews DC, Ganzer C, Osorio RS, Isaacson RS, De Leon MJ, Convit A. Lifestyle and vascular risk effects on MRI-based biomarkers of Alzheimer's disease: a cross-sectional study of middle-aged adults from the broader New York City area. *BMJ Open* 2018;**8**:e019362.
23. Gorelick PB, Sorond F. Vascular risk burden, brain health, and next steps. *Neurology* 2018;**91**:729–730.
24. Barnes DE, Yaffe K. The projected effect of risk factor reduction on Alzheimer's disease prevalence. *Lancet Neurol* 2011;**10**:819–828.
25. Pase MP, Davis-Plourde K, Himali JJ, Satizabal CL, Aparicio H, Seshadri S, Beiser AS, DeCarli C. Vascular risk at younger ages most strongly associated with current and future brain volume. *Neurology* 2018;**91**:e1479–e1486.
26. Pedditzi E, Peters R, Beckett N. The risk of overweight/obesity in mid-life and late life for the development of dementia: a systematic review and meta-analysis of longitudinal studies. *Age Ageing* 2016;**45**:14–21.
27. Alfaro-Almagro F, Jenkinson M, Bangerter NK, Andersson JLR, Griffanti L, Douaud G, Sotiropoulos SN, Jbabdi S, Hernandez-Fernandez M, Vallee E, Vidaurre D, Webster M, McCarthy P, Rorden C, Daducci A, Alexander DC, Zhang H, Dragonu I, Matthews PM, Miller KL, Smith SM. Image processing and quality control for the first 10,000 brain imaging datasets from UK Biobank. *Neuroimage* 2018;**166**:400–424.
28. Cox SR, Ritchie SJ, Tucker-Drob EM, Liewald DC, Hagenaars SP, Davies G, Wardlaw JM, Gale CR, Bastin ME, Deary IJ. Ageing and brain white matter structure in 3,513 UK Biobank participants. *Nat Commun* 2016;**7**:13629.
29. Penke L, Maniega SM, Murray C, Gow AJ, Valdes Hernandez MC, Clayden JD, Starr JM, Wardlaw JM, Bastin ME, Deary IJ. A general factor of brain white matter integrity predicts information processing speed in healthy older people. *J Neurosci* 2010;**30**:7569–7574.
30. Telford EJ, Cox SR, Fletcher-Watson S, Anblagan D, Sparrow S, Pataky R, Quigley A, Semple SI, Bastin ME, Boardman JP. A latent measure explains substantial variance in white matter microstructure across the newborn human brain. *Brain Struct Funct* 2017;**222**:4023–4033.
31. National Health Service. What is the body mass index (BMI)? http://www.nhs.uk/chq/Pages/3215.aspx? CategoryID= 52 (30 November 2018).
32. World Health Organisation. Body mass index - BMI. http://www.euro.who.int/en/health-topics/disease-prevention/nutrition/a-healthy-lifestyle/body-mass-index-bmi (30 November 2018).
33. World Health Organisation. Waist circumference and waist-hip-ratio: report of a WHO expert consultation. http://apps.who.int/iris/bitstream/10665/44583/1/9789241501491_eng.pdf (30 November 2018).
34. Wardlaw JM, Allerhand M, Doubal FN, Valdés Hernández MC, Morris Z, Gow AJ, Bastin ME, Starr JM, Dennis MS, Deary IJ. Vascular risk factors, large-artery atheroma, and brain white matter hyperintensities. *Neurology* 2014;**82**:1331–1338.
35. Hull JG, Tedlie JC, Lehn DA. Moderator variables in personality research: the problem of controlling for plausible alternatives. *Pers Soc Psychol Bull* 1992;**18**:115–117.
36. Yzerbyt VY, Muller D, Judd CM. Adjusting researchers' approach to adjustment: on the use of covariates when testing interactions. *J Exp Soc Psychol* 2004;**40**:424–431.
37. Benjamini Y, Hochberg Y. Controlling the false discovery rate: a practical and powerful approach to multiple testing. *J R Stat Soc B* 1995;**57**:289–300.
38. Cohen J. A power primer. *Psychol Bull* 1992;**112**:155–119.
39. Hewitt J, Walters M, Padmanabhan S, Dawson J. Cohort profile of the UK Biobank: diagnosis and characteristics of cerebrovascular disease. *BMJ Open* 2016;**6**:e009161.
40. Miller KL, Alfaro-Almagro F, Bangerter NK, Thomas DL, Yacoub E, Xu J, Bartsch AJ, Jbabdi S, Sotiropoulos SN, Andersson JLR, Griffanti L, Douaud G, Okell TW, Weale P, Dragonu I, Garratt S, Hudson S, Collins R, Jenkinson M, Matthews PM, Smith SM. Multimodal population brain imaging in the UK Biobank prospective epidemiological study. *Nat Neurosci* 2016;**19**:1523–1536.
41. Ritchie SJ, Cox SR, Shen X, Lombardo MV, Reus LM, Alloza C, Harris MA, Alderson HL, Hunter S, Neilson E, Liewald DCM, Auyeung B, Whalley HC, Lawrie SM, Gale CR, Bastin ME, McIntosh AM, Deary IJ. Sex differences in the adult human brain: evidence from 5216 UK Biobank participants. *Cereb Cortex* 2018;**28**:2959–2975.
42. Dickie DA, Karama S, Ritchie SJ, Cox SR, Sakka E, Royle NA, Aribisala BS, Valdés Hernández MC, Muñoz Maniega S, Pattie A, Corley J, Starr JM, Bastin ME, Evans AC, Deary IJ, Wardlaw JM. Progression of white matter disease and cortical thinning are not related in older community-dwelling subjects. *Stroke* 2016;**47**:410–416.
43. Tuladhar AM, Reid AT, Shumskaya E, de Laat KF, van Norden AGW, van Dijk EJ, Norris DG, de Leeuw F-E. Relationship between white matter hyperintensities, cortical thickness and cognition. *Stroke* 2015;**46**:425–432.
44. Payabvash S, Souza LCS, Wang Y, Schaefer PW, Furie KL, Halpern EF, Gonzalez RG, Lev MH. Regional ischemic vulnerability of the brain to hypoperfusion: the need for location specific CT perfusion thresholds in acute stroke patients. *Stroke* 2011;**42**:1255–1260.
45. Ferreira D, Verhagen C, Hernández-Cabrera JA, Cavallin L, Guo C-J, Ekman U, Muehlboeck J-S, Simmons A, Barroso J, Wahlund L-O, Westman E. Distinct subtypes of Alzheimer's disease based on patterns of brain atrophy: longitudinal trajectories and clinical applications. *Sci Rep* 2017;**7**:46263.
46. Bartzokis G, Sultzer D, Lu PH, Nuechterlein KH, Mintz J, Cummings JL. Heterogeneous age-related breakdown of white matter structural integrity: implications for cortical 'disconnection' in aging and Alzheimer's disease. *Neurobiol. Aging* 2004;**25**:843–851.
47. Hilal S, Amin SM, Venketasubramanian N, Niessen WJ, Vrooman H, Wong TY, Chen C, Ikram MK. Subcortical atrophy in cognitive impairment and dementia. *J Alzheimers Dis* 2015;**48**:813–823.
48. Bray GA, K.K. Kim JPH; Wilding & World Obesity Federation. Obesity: a chronic relapsing progressive disease process. A position statement of the World Obesity Federation. *Obes. Rev* 2017;**18**:715–723.
49. Talukder MAH, Johnson WM, Varadharaj S, Lian J, Kearns PN. Chronic cigarette smoking causes hypertension, increased oxidative stress, impaired NO bioavailability, endothelial dysfunction, and cardiac remodelling in mice. *Am J Physiol Heart Circ Physiol* 2011;**3000**:H388–H396.
50. Lyall DM, Cox SR, Lyall LM, Celis-Morales C, Cullen B, Mackay DF, Ward J, Strawbridge RJ, McIntosh AM, Sattar N, Smith DJ, Cavanagh J, Deary IJ, Pell JP. Association between APOE e4 and white matter hyperintensity volume, but not total brain volume or white matter integrity. *Brain Imaging Behav*;doi: 10.1007/s11682-019-00069-9.
51. Fry A, Littlejohns TJ, Sudlow C, Doherty N, Adamska L, Sprosen T, Collins R, Allen NE. Comparions of sociodemographic and health-related characteristics of UK Biobank participants with those of the general population. *Am J Epidemiol* 2017;**186**:1026–1034.
52. Cox SR, Ritchie SJ, Dickie DA, Pattie A, Royle NA, Corley J, Aribisala BS, Harris SE, Valdés Hernández M, Gow AJ, Muñoz Maniega S, Starr JM, Bastin ME, Wardlaw JM, Deary IJ. Interaction of *APOE* e4 and poor glycemic control predicts white matter hyperintensity growth from 73 to 76. *Neurobiol Aging* 2017;**54**:54–58.
53. Nation DA, Preis SR, Beiser A, Bangen KJ, Delano-Wood L, Lamar M, Libon DJ, Seshadri S, Wolf PA, Au R. Pulse pressure is associated with early brain atrophy and cognitive decline: modifying effects of *APOE* e4. *Alzheimer Dis Assoc Disord* 2016;**30**:210–215.
54. Jones DK, Knösche TR, Turner R. White matter integrity, fiber count, and other fallacies: the dos and don'ts of diffusion MRI. *Neuroimage* 2013;**73**:239–254.